ARCHIVIO ISTITUZIONALE
DELLA RICERCA

Alma Mater Studiorum Università di Bologna
Archivio istituzionale della ricerca

Stimulated x-ray Raman scattering for selective preparation of dark states bypassing optical selection rules

This is the final peer-reviewed author's accepted manuscript (postprint) of the following publication:

Published Version:
Montorsi, F., Mukamel, S., Tamassia, F., Garavelli, M., Segatta, F., Nenov, A. (2025). Stimulated x-ray Raman scattering for selective preparation of dark states bypassing optical selection rules. PHYSICAL REVIEW A, 111(6), 1-11 [10.1103/2lfz-pqzt].

Availability:
This version is available at: https://hdl.handle.net/11585/1028440 since: 2025-11-09

Published:

DOI: http://doi.org/10.1103/2lfz-pqzt

Terms of use:

Some rights reserved. The terms and conditions for the reuse of this version of the manuscript are specified in the publishing policy. For all terms of use and more information see the publisher's website.

This item was downloaded from IRIS Università di Bologna (https://cris.unibo.it/).
When citing, please refer to the published version.

(Article begins on next page)

16 November 2026

Stimulated X-ray Raman scattering for selective preparation of *dark* states bypassing optical selection rules

Francesco Montorsi, Filippo Tamassia, Marco Garavelli, Francesco Segatta,* and Artur Nenov†
Dipartimento di Chimica Industriale "Toso Montanari", Università di Bologna - Alma Mater Studiorum, Via Piero Gobetti 85, 40129 - Bologna, Italy

Shaul Mukamel
Department of Chemistry and Department of Physics and Astronomy, University of California, Irvine, 92697, USA

We present an X-ray based stimulated Raman approach to control the preparation of populations and coherent superpositions of (valence) electronic states in generic molecular systems, including optically dark states. Leveraging on the unique properties of core-level excitations as intermediates of the Raman process, we demonstrate that optically forbidden singlet-singlet and singlet-triplet transitions are made accessible. We explore the role of both intrinsic molecular properties (transition dipole moments/involved molecular orbitals) and external field parameters to explain the efficiency and selectivity of the process towards specific classes of electronic states, and to control it towards the amplification of desired populations/superpositions. While the reported mechanism naturally apply to virtually all organic/bio-organic molecules and can straightforwardly be extended to a broader class of molecules, atoms and materials, detailed results for two molecular systems are here reported as a test-bed of the proposed approach, for which experimental feasibility is eventually discussed.

I. INTRODUCTION

Light-matter interaction is a fundamental process that has been extensively exploited to study, prepare and manipulate the evolution of desired quantum state(s) or superpositions thereof in atoms, molecules and materials. A variety of photon energies can be employed, from the infrared to X-rays, triggering diverse phenomena. The creation of the desired state/superposition via single-photon processes imposes the following requirements on the initial and final states: a) their energy difference needs to match the energy of the incident photon; b) the transition needs to be dipole-allowed. While the first requirement can be satisfied by manipulating the laser source, the fulfillment of the second one depends on an intrinsic property of the system, i.e., the (transition) dipole moment.

Materials often exhibit valence electronic excited states which are termed *dark*, i.e., states that are not (or only weakly) dipole-coupled to the ground state and thus cannot undergo efficient single-photon absorption/emission. These could be states which exhibit spin change, charge transfer character or for which the transition dipole moment integral is zero by symmetry. Yet, being dark does not render such states *insignificant*: lacking the emission channel they can acquire extremely long lifetime and be protected from the environment, a fact that make them potentially interesting for molecular photocatalysis and quantum information applications.[1] Moreover, they are known to mediate electronic population transfer in a large variety of organic/bio-organic molecules, being involved in ultra-fast internal conversion[2, 3], energy and charge transfer,[4] photoredox catalysis, photo-damage and thermally induced delayed fluorescence.[5, 6] Among the most prominent examples are DNA and RNA, where the role of dark states is still debated in light of their potential ability to impair such molecules photo-protection mechanism.[7–10]

Preparing, manipulating, and tracking the evolution of dark states is therefore of utmost interest. Achieving this using *standard* spectroscopic techniques can be quite challenging, if not entirely unfeasible, particularly when states with different spin multiplicities are involved. Transient absorption and photo-electron spectroscopy allows to track the fate of dark states as long as they give rise to absorption features in a background free spectral window. However, the inability to prepare selectively a dark state makes it difficult to identify its spectroscopic fingerprints next to those of the bright states. In this letter we show that stimulated X-ray Raman scattering (SXRS), one of the promising nonlinear X-ray techniques enabled by XFEL facilities,[11–16] can be employed to selectively prepare molecular systems into a singlet or triplet dark quantum state. To achieve this goal, we rely on dipole-coupling between valence and core-excited states, characterized by different selection rules with respect to *optical* (UV/Vis) transitions. As it will be shown, such different selection rules leverage on the site specificity and locality of core-level transitions. By controlling the Raman field properties, such as the field(s) central frequency, width and shape, additional selectivity towards desired states can be achieved.

Notably, this scheme can be used to create coherent superpositions of dark and non-dark (termed *bright*) electronic states, as, e.g, singlet-singlet, singlet-triplet and triplet-triplet coherences, opening the possibility to study uncommon and otherwise elusive states of matter.

In this manuscript we explore the capabilities, re-

* francesco.segatta@unibo.it
† artur.nenov@unibo.it

quirements and limitations of SXRS to produce desired states/superpositions on two molecular systems, namely: *trans*-azobenzene, for which we demonstrate that the dark (singlet) $n\pi^*$ state can be populated with a near 100% selectivity via nitrogen K-edge transitions, and thio-formaldehyde, for which we show the ability to selectively target states from the triplet manifold via the $L_{2,3}$-edge of sulfur. Comparison of the Raman process efficiency at different elements edges (K-edge, L_1-edge) will be also discussed.

II. CONCEPT AND METHODOLOGY

A. Stimulated X-ray Raman Scattering

Let us consider the three manifolds of states involved in the Raman process, namely, $\mathcal{G}$ (ground state), $\mathcal{E}$ (valence excited manifold), and $\mathcal{C}$ (core-excited manifold). We will indicate states of $\mathcal{G}$, $\mathcal{E}$ and $\mathcal{C}$ manifolds with the indexes g, e and c, respectively. Let us denote the transition dipole moment between the generic states a and b as $\boldsymbol{\mu}_{ab}$. The *brightness* of a $g \rightarrow e$ transition is proportional to the magnitude of the associated transition dipole moment $\boldsymbol{\mu}_{ge}$. Such transitions might be forbidden in direct one-photon absorption due to: (i) spin change (e.g., singlet to triplet transitions); (ii) vanishingly small *spatial overlap* between the orbitals involved in the transition[17] (e.g., charge transfer transitions); (iii) symmetry restrictions (e.g., $n \rightarrow \pi^*$ transitions present in many conjugate and aromatic organic molecules). SXRS, at variance, involves intermediate core excited states coupled to the $\mathcal{G}$ and $\mathcal{E}$ manifolds over the transition dipoles $\boldsymbol{\mu}_{gc}$ and $\boldsymbol{\mu}_{ce}$ whose magnitude is dictated by the extent of the *spatial overlap* of the highly localized *core* orbital (χ_c) and the delocalized *virtual valence* orbitals (χ_{v^*}) and by the *local* symmetry around the atomic core-hole site[3, 18]. SXRS can be described as a two step process[19]: a first interaction with the X-ray field (named *pump*) promotes an electron from χ_c to χ_{v^*}, populating a core excited state denoted as $\chi_c^{[1]}\chi_{v^*}^{[1]}$ (molecular orbital occupation highlighted in the square brackets). A second interaction with the X-ray field (named *stokes*) drives an electron from an *occupied valence* orbital (χ_v) into the core vacancy, resulting in the generation of a valence excited (e) state $\chi_v^{[1]}\chi_{v^*}^{[1]}$ (a graphical description of this scheme is reported in Figure 1-(c), which also shows prototypical n, π and π^* frontier orbitals of organic molecular systems). SXRS can thus be exploited to populate valence excited states via a (Raman) pathway $g \rightarrow c \rightarrow e$ that can bypass selection rules of the direct $g \rightarrow e$ process.

Two mechanisms for populating (dark) singlet or triplet states will be considered, as depicted in the schematic of Figure 1-(a) and (b), respectively: i) the s-core mechanism, which takes advantage of the allowed transitions between the spherically symmetric 1s or 2s core orbitals and all types of valence orbitals (π, π^*, n, σ, σ^*, Rydberg) to promote the population of dark valence states; and ii) the p-core mechanism, for which the selective population of valence triplet states can be demonstrated, capitalizing on the strong singlet-triplet mixing of p orbitals at the $L_{2,3}$-edge[20].

One should note that symmetry forbidden transitions to dark singlet states can acquire slight brightness due to vibronic coupling (so-called vibronic borrowing). Still, the resulting transition to those states will be weak, and their direct excitation will be achieved only when there is no background from brighter transitions. By leveraging on the local symmetry around the core-hole, the indirect SXRS process allows to overcome the symmetry selection rules and selectively populate dark singlet states also when their band overlap with bright states transitions. Transitions to triplet states in the $\mathcal{E}$ manifold might be also accessible through a direct process in case of a large spin-orbit couplings (as exhibited, for example, in metal-organic complexes). This effect is manifested when the charge of the nuclei constituting the molecule are large enough to induce relativistic effects. However, the vast majority of organic molecules are characterized by atoms with relatively low nuclear charge, so that only very few of them display a significant spin-orbit coupling among the valence states. Third (or higher) row elements have access to the $L_{2,3}$-edge states which are characterized by a pronounced spin-orbit coupling (up to hundreds of meV) due to the direct involvement of (*strongly coupled*) inner shell $2p$ orbitals. Utilizing $L_{2,3}$-edge states as intermediates in the SXRS process makes it possible to bypass the spin selection rule, by creating a superposition of core-excited states with different spin via the *pump* interaction, which can than be selectively converted to pure triplet valence state via the *stokes* interaction (see Figure 1-(b)). In this case χ_c corresponds to a triad of $2p$ orbitals (i.e., $2p_x$, $2p_y$ and $2p_z$) whose different orientation in the 3D space gives rise to a complex set of system-dependent selection rules, that are discussed in the Supplemental Material.[21]

B. Simulation methodology

High level ab-initio electronic structure calculations, based on multi-reference wave function theory (XMS-RASPT2)[22, 23] were performed to obtain the valence and core-excited singlet and triplet manifolds of states as well as the transition dipole moments between such manifolds[24], taking into account scalar relativistic effects[25] and evaluating the spin-orbit coupling for the core excited states contributing to the $L_{2,3}$-edge[26]. All calculations were performed with the quantum chemistry software OpenMolcas.[27–29] Details about the computational protocol are reported in the Supplemental Material.[21]

The system field-driven dynamics during the SXRS process has been simulated solving the time-dependent Schrödinger equation for the electronic degrees of free-

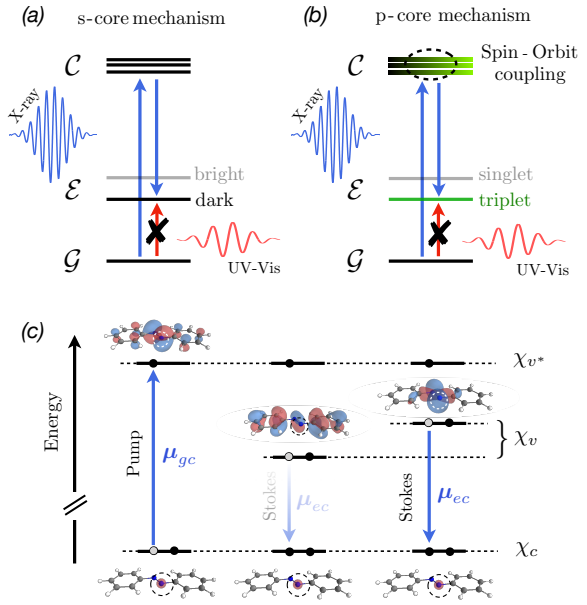

FIG. 1. Schematic of the proposed SXRS mechanism: (a) *s*-core mechanism utilizing *s*-type core orbitals as a gateway for the population of dark singlet states in the valence manifold $\mathcal{E}$; (b) *p*-core mechanism via the $L_{2,3}$-edge, to selectively populate valence excited triplet states exploiting singlet-triplet mixing in the core-excited state manifold; (c) Molecular orbital view of the process, with *pump* and *stokes* interaction involving the prototypical valence orbitals of organic molecular systems. Notably, the intensities of the transitions depend on the spatial overlap between core and valence orbitals (e.g., $n \to 1s$ is typically more intense than $\pi \to 1s$).

dom through the QuTiP python package[30, 31], explicitly including the field-matter interaction term in the system Hamiltonian, which reads

$$\hat{H} = \hat{H}_0 + \hat{H}_{\text{int}}(t) \tag{1}$$

Here, $\hat{H}_0$ represents the molecular (electronic) Hamiltonian, that can be written highlighting the electronic states of the three considered manifolds, i.e.

$$\hat{H}_0 = \epsilon_g |g\rangle\langle g| + \sum_{e\in\mathcal{E}} \epsilon_e |e\rangle\langle e| + \sum_{c\in\mathcal{C}} \epsilon_c |c\rangle\langle c| \tag{2}$$

ϵ_a being the energy of the generic state a; $\hat{H}_{\text{int}}$ is the time-dependent field-matter interaction term, which reads

$$\hat{H}_{\text{int}}(t) = -\hat{\boldsymbol{\mu}} \cdot \hat{\boldsymbol{\epsilon}} E(t) \tag{3}$$

where $\hat{\boldsymbol{\mu}}$ is the transition dipole moment operator, $\hat{\boldsymbol{\epsilon}}$ and $E(t)$ are the X-ray field polarization vector and time domain functional form, respectively. The latter is typically given by the product of a time envelope $\mathcal{E}(t)$ and a cosine function ($\mathcal{E}(\omega)$ similarly defines the field envelope in the frequency domain).

Two X-ray field setups were considered to promote the stimulated Raman process: a single broadband (Gaussian shaped) X-ray pulse, whose technical feasibility to promote SXRS was recently demonstrated by Cryan and co-workers[32]), and a pair of narrow-band (Gaussian shaped) X-ray pulses with adjustable central frequencies and intensities to maximize the Raman efficiency of the desired process. The fields are centered at time zero, and their functional form in the time domain reads:

$$\begin{aligned} E_{\text{sing}}(t) &= \mathcal{E}_0(t)\left(e^{-i\omega_0 t} + e^{+i\omega_0 t}\right) \\ E_{\text{pair}}(t) &= \mathcal{E}_p(t)\left(e^{-i\omega_p t} + e^{+i\omega_p t}\right) + \\ &+ \mathcal{E}_s(t)\left(e^{-i\omega_s t} + e^{+i\omega_s t}\right) \end{aligned}$$

where the subscript p and s stands for pump and stokes, respectively; $\mathcal{E}_j(t) = \mathcal{E}_j \exp\left(-\frac{t^2}{2\sigma_t^2}\right)$ is the field envelope in the time-domain, $\mathcal{E}_0$, $\mathcal{E}_p$ and $\mathcal{E}_s$ are the field amplitudes, ω_0, ω_p and ω_s are the pulses central frequencies, and σ_t is the time-domain standard deviation of the gaussian shaped pulse(s).

The performed field-matter interaction calculations are non-perturbative. Population decay and coherence dephasing terms are assumed to be negligibly small in the few-fs time-scales explored. Moreover, efficiency losses via ionization channels were not considered in this exploratory work (see the Supplemental Material[21] for additional details).

C. Perturbative analysis and key processes

While all simulations reported in this letter are fully non-perturbative, analyzing expressions obtained via perturbation expansion of the molecular density matrix $\hat{\varrho}(t)$ in powers of the X-ray field[33] allows to highlight the key factors influencing a given process. In particular, we focused on two light-induced processes: a) generation of a coherence (ϱ_{eg}) between the ground state and a valence excited state, which is effectively described by second-order perturbation theory; b) generation of a valence state population (ϱ_{ee}) where a perturbation expansion of the molecular density matrix up to the fourth-order is required. [34]

Let us denote with ω_{ab} the transition energy between electronic states a and b, where a and b are generic labels comprising the states from each of the three manifold of states here considered ($\mathcal{G}$, $\mathcal{E}$ and $\mathcal{C}$). The perturbative expression for the coherence prepared by the SXRS, in the dipole approximation[35], reads:

$$\varrho_{eg}^{(2)}(t) = -\frac{i}{\hbar^2} e^{-i\tilde{\omega}_{ge}t} \alpha_{eg}^{(2)} \tag{4}$$

where the term $\alpha_{eg}^{(2)}$ is the $e-g$ matrix element of the molecular polarizability operator $\hat{\alpha}$. $\tilde{\omega}_{ab} = \omega_{ab} - i\gamma_{ab}/2$ denotes the complex $a-b$ frequency with γ_{ab} the $a-b$ coherence dephasing time. Working in the impulsive limit (ISXRS), where all the required field matter interactions occur under the envelop of the same attosecond X-ray pulse, the polarizability expression for a single broad-

band pulse reads:

$$\alpha^{(2)}_{eg} = \sum_c (\hat{\boldsymbol{\epsilon}}^* \cdot \boldsymbol{\mu}_{ec})(\hat{\boldsymbol{\epsilon}} \cdot \boldsymbol{\mu}^\dagger_{gc}) \int_{-\infty}^{+\infty} \frac{d\omega}{2\pi} \frac{\mathcal{E}(\omega)\mathcal{E}^*(\omega - \omega_{ge})}{\omega + \omega_0 - \tilde{\omega}_{gc}} \tag{5}$$

If the field is given by the two (time coincident) narrow-band pulses, the expression above can be rewritten as:

$$\alpha^{(2)}_{eg} = \sum_c (\hat{\boldsymbol{\epsilon}}^* \cdot \boldsymbol{\mu}_{ec})(\hat{\boldsymbol{\epsilon}} \cdot \boldsymbol{\mu}^\dagger_{gc}) \int_{-\infty}^{+\infty} \frac{d\omega}{2\pi} \frac{\mathcal{E}_p(\omega)\mathcal{E}^*_s(\omega - \omega_{ge} + \Delta)}{\omega + \omega_p - \tilde{\omega}_{gc}} \tag{6}$$

where the pump and stokes subscripts explicitly appear, and $\Delta = \omega_p - \omega_s$. Assuming Gaussian shaped pulse envelopes and a single relevant core-excited state in the $\mathcal{C}$ manifold (which is the case for both systems explored in this work), a simple condition on the central frequencies of the field(s) can be obtained (in the perturbative limit) to maximize the coherence amplitude. For the single broadband pulse, the pulse central frequency ω_0 should be half-way between the two relevant ($g - c$ and $e - c$) gaps; for the narrow-band pulse pair, the pump and stokes pulses should be centered to their respective energy gaps. If multiple core-excited states are accessed during the process, the central frequency(ies) is determined by a weighted average over the various $g - c$ and $e - c$ gaps.

Similar polarizability expressions (and optimal central frequency values) can be derived for the population term $\varrho_{ee}(t)$ (see Supplemental Material for both final expressions and derivation[21]).

III. RESULTS

SXRS induced coherences and populations of the $n\pi^*$ azobenzene state, as well as the thio-formaldehyde triplet states are reported below for both field setups. For the single broadband pulse, a pulse FWHM of 0.5 fs (corresponding to $\sigma_t = 0.21$ fs) was employed, together with a field amplitude of $\mathcal{E}_0 = 17.0$ GV cm^{-1} (and thus a peak intensity $I_0 = 3.8 \times 10^{17}$ Wcm^{-2}), parameters set to mimic the ones of ref. 32. The central frequency value ω_0 was optimized to maximize the population of the states of interest. For the pair of narrow-band pulses, longer 5 fs FWHM ($\sigma_t = 2.1$ fs) pulses were employed; the pump and stokes central frequencies were set to match $g-c$ and $c-e$ energy gaps, respectively, while the intensities were tuned to obtain a local maximum in the desired e state population (with an optimization procedure described in the Supplemental Material [21]). All field parameters are specified in Table III C.

A. Population of (dark) singlet states

We first consider *trans*-azobenzene, for which we demonstrate the s-core mechanism to populate its dark $n\pi^*$ state. A schematic description of its electronic structure is reported in Figure 2-(a). Azobenzene exhibits a dark $n\pi^*$ state placed around 2.7 eV, and a bright $\pi\pi^*$ state around 4.0 eV which dominates its linear absorption spectrum[2]. In the following we explore the ISXRS process employing a single attosecond pulse (Figure 2-(b)) resonant with the nitrogen K-edge ($\omega_0 = 397.5$ eV) which selectively prepares the dark $n\pi^*$ state in a two-step process $1s^{[2]}n^{[2]}\pi^{*[0]} \rightarrow 1s^{[1]}n^{[2]}\pi^{*[1]} \rightarrow 1s^{[2]}n^{[1]}\pi^{*[1]}$. This is documented in Figure 2-(d) which shows the time evolution of coherence term $\varrho_{eg}(t)$, with e being either the $\pi\pi^*$ or the $n\pi^*$ state. Notably, at the end of the light-matter interaction, the value of the coherence $\varrho_{eg}(t)$ involving the $n\pi^*$ state is about one order of magnitude larger than the one involving the $\pi\pi^*$ state. A similar trend is observed when computing the excited state populations $\varrho_{ee}(t)$, as reported in Figure 2-(c). The $n\pi^*$ population amounts to about 3.5% of the initial ground state population, while the $\pi\pi^*$ population is about two orders of magnitude lower. Selectivity towards the dark state is achieved exploiting the different extent of localization of the n and π orbitals on top of the nitrogen atom, which give rise to extremely low $\boldsymbol{\mu}_{ce}$ for the $\pi\pi^*$ state. This key observation is examined in details and generalized in the Discussion section.

B. Population of triplet states

Direct population of electronically excited states involving spin change is a much harder challenge since one-photon absorption is forbidden for these states by the so-called spin selection rule. The population of triplet states via the p-core mechanism is here demonstrated on the example of thio-formaldehyde. Its manifold of low-lying electronic states consists of a singlet (S_1) state of $n\pi^*$ character positioned in between two triplet states (T_1 and T_2) of $n\pi^*$ and $\pi\pi^*$ character, respectively (Figure-2-(e)). States in the $\mathcal{E}$ manifold display an almost negligible spin-orbit coupling, making the direct population of the aforementioned triplet states virtually impossible. Strong relativistic effects are manifest at the sulfur $L_{2,3}$-edge, leading to large core-state singlet/triplet mixing which enables access to the valence triplet manifold over the indirect (Raman) pathway.

Figure 2 reports the results obtained solving the time-dependent Schrödinger equation in the same condition discussed in the previous example, employing a single X-ray pulse near resonant with the sulfur $L_{2,3}$-edge ($\omega_0 = 160.0$ eV). Figure 2-(h) shows the $\varrho_{eg}(t)$ prepared by the ISXRS process, demonstrating the possibility to create a coherence between the (singlet) ground state and the valence-excited triplet states. Notably, $g - T_1$ and $g - T_2$ coherences are prepared without any background from the S_1 state (see the Supplemental Material[21] for additional details). A similar trend is observed when creating population in the triplet states, as evidenced in Figure 2-(g). The low population achieved in this case

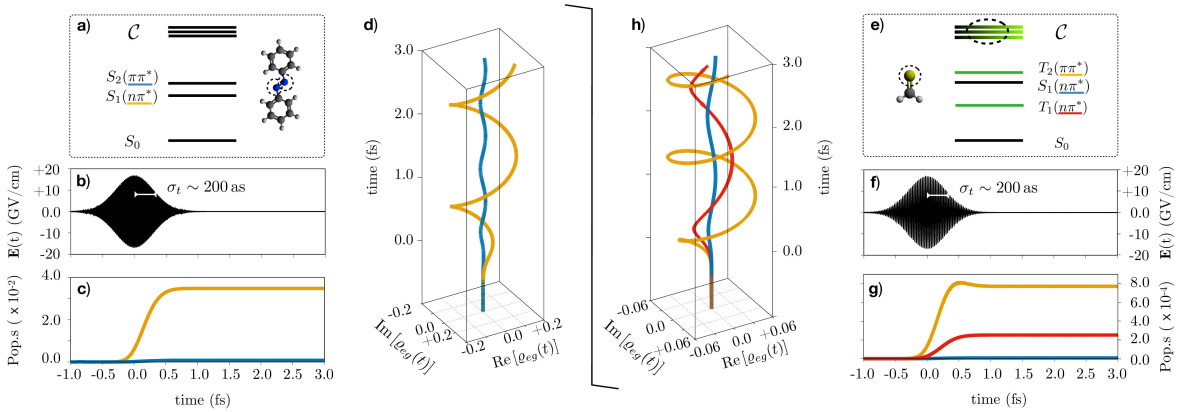

FIG. 2. Examples of s-core and p-core mechanisms for dark singlet and triplet valence excited state preparation. (a/e) Scheme of the *trans*-azobenzene and thio-formaldehyde electronic structure. (b/f) Broadband Gaussian shaped X-ray field used to induce the impulsive SXRS process. (c/g) Evolution of the excited state populations $\varrho_{ee}(t)$ during and after the interaction with the X-ray pulse. (d/h) Evolution of the (complex valued) coherences $\varrho_{eg}(t)$. Throughout the figure, energy levels, populations and coherences involving the various excited states are consistently depicted with different colors.

(∼0.1% and ∼0.02% for T_1 and T_2 states, respectively) is ascribed to the low values of the thio-formaldehyde core-to-valence transition dipole moments, calling for a manipulation of the X-ray field that drives the process to achieve higher efficiencies.

C. Controlling efficiency via field manipulation

While the results reported above demonstrate the viability of the proposed s-core and p-core mechanisms to prepare (dark) singlet and triplet valence states via a single broadband pulse, the relatively low process efficiency is apparent. In this section we explore an alternative two narrow-band pulses setup as the simplest form of field manipulation to improve the efficiency and the state selectivity.

Figure 3-a) shows the higher efficiency of the two narrow-band pulses setup on the azobenzene example, where an order of magnitude higher population of the targeted $n\pi^*$ state is observed, with a final population of about 40%. The central frequencies of the (weaker) pump and the (stronger) probe are set to match the $g-c$ and $c-e$ gaps, respectively (see Figure 3-b)). Notably, the peak-intensity of both pump and stokes is weaker with respect to the one employed in the single broadband pulse case.

Figure 3-c)/d) demonstrate, on the example of thio-formaldehyde, the possibility of selective enhancement of the desired triplet state population, achieved by properly tuning the central frequencies of the stokes pulse to resonate with either of the two non-degenerate triplets. Again, a much higher efficiency is obtained for both states, with ca. 3% and 9% population for T_1 and T_2, respectively, and a negligible population of the other state, employing fields peak intensities lower than in the single broadband pulse setup. A much weaker stokes pulse is employed for optimizing the population of the T_2 state since $|\boldsymbol{\mu}_{cT_2}| > |\boldsymbol{\mu}_{cT_1}|$.

	$n\pi^*$ azo		Opt. T_1 thio		Opt. T_2 thio	
	pump	stokes	pump	stokes	pump	stokes
$\omega_{p/s}$ (eV)	398.8	396.2	161.25	159.45	161.25	157.85
$\mathcal{E}_{p/s}$ (GV cm^{-1})	1.36	5.66	6.99	7.97	6.99	8.48

TABLE I. Values of the pump and stokes central frequencies and field amplitudes. A common FWHM of 5 fs ($\sigma_t \sim 2.1$ fs) has been employed, which corresponds to a pulse of 0.24 eV FWHM in the frequency domain.

IV. DISCUSSION

A. Molecular orbital interpretation of state selectivity

Let us explore the two mechanisms proposed above from a molecular orbital point of view, that allows to clarify the efficiency of the process for different classes of states. In the *s*-core mechanism, χ_c is a $1s$ (or a $2s$) orbital whose spherical shape guarantees symmetry allowed transitions toward any kind of orbital having contribution from *p*-type basis functions. Valence *frontier* orbitals in organic molecules ($v \in \{\sigma, \pi, n\}$; $v^* \in \{\sigma^*, \pi^*\}$) are mainly described by linear combination of p atomic orbitals making all core transitions allowed. Therefore, the magnitude of both $\boldsymbol{\mu}_{gc}$ and $\boldsymbol{\mu}_{ce}$ is essentially dictated by the *spatial overlap* between the valence molecular orbitals and the *s*-core orbitals: it is larger for valence orbitals with significant MO coefficients at the core-excited atoms (such as lone pairs localized on heteroatoms), and smaller for valence orbitals delocalized over large portions of the molecular system (such as σ/σ^* and π/π^* orbitals).

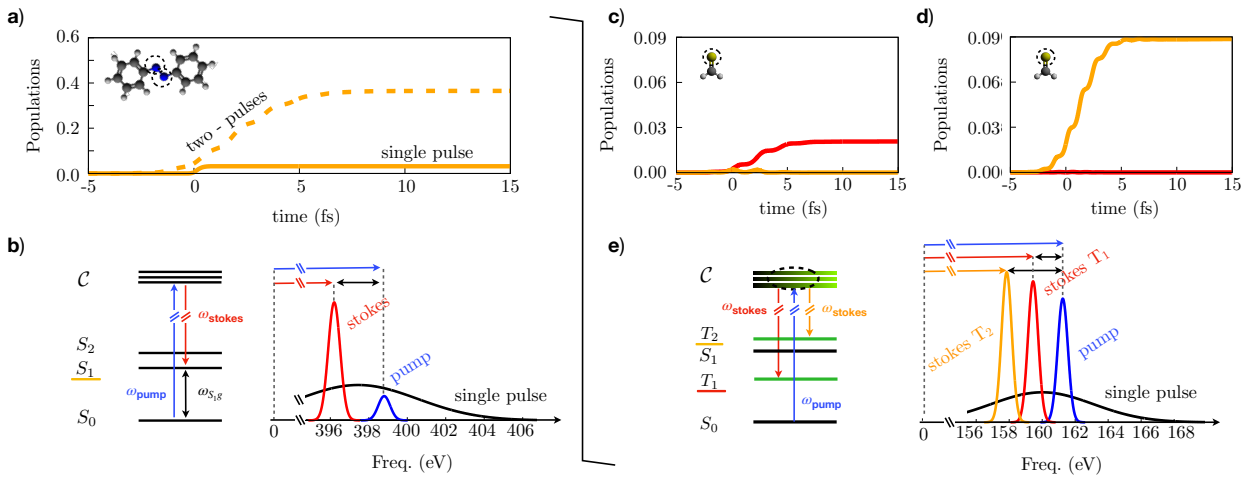

FIG. 3. a) Efficiency of single broadband vs two narrow-band SXRS pulses in promoting the population of the dark $n\pi^*$ azobenzene singlet state. The two-pulses setup achieves 40% of $n\pi^*$ population (while only 3.5% is achieved in the single pulse setup) b) energy level diagram and matching between energy gaps and pump/stokes pulses central frequencies (field reported in the frequency domain); c/d) Ability of SXRS with two narrow-band pulses to selectively promote the population of a specific triplet state in thio-formaldehyde. The efficiency of this setup with respect to the single broadband pulse setup is also orders of magnitude higher (∼3% and ∼9% population for T_1 and T_2 populations, respectively); e) same of b), but for the two different pathways to maximize the coherence/population of each of the triplet states in thio-formaldehyde.

Considering transitions from the more extended 2s orbitals in comparison with the more compact 1s orbitals is expected to give rise to larger spatial overlaps, and thus to larger transition dipole moments at the L_1-edge with respect to those at the K-edge. Indeed, calculations performed at the sulfur K- and L_1-edges (as reported in the Supporting Material for the sulfur atom edges in thio-formaldehyde[21]) show that the relevant transition dipole moments are a few orders of magnitude larger for the latter.

The observation made is quite general and not limited to the system studied here, as it leverages on the peculiar nature of core-level excitations that can be exploited to selectively control the final state produced by the SXRS process. In particular, it suggests to use the K-edge/L_1-edge of heteroatoms as the gateway to selectively access (typically dark) $n\pi^*$ states.

For what concerns the p-core mechanism, the explanation of the transition brightness is less trivial, and an exhaustive discussion is reported in the Supplemental Material [21]. It is worth noticing that p→p transitions are forbidden, and thus the transition from the 2p core orbitals to the π^* orbital is mainly due to the minor admixture of d atomic orbitals. Interestingly, this means that the brightest transitions involving the 2p electrons are to be expected to and from orbitals of pronounced s and d character, i.e. on orbitals predominantly localized on the third-row element itself.[36]

B. Improving efficiency and selectivity via field control

Let us analyze the two different field setups employed in the simulations. In the case of the single broadband pulse, it is clear that the minimal requirement to promote the desired SXRS process is to have a bandwidth grater than the energy gap between the ground and the desired valence e state (see eq. 6). If the $e-g$ gap exceeds the field bandwidth, the Raman process to that state will be unproductive. Scans over the field central frequency identified the optimal ω_0 value in close agreement to the perturbative prediction, setting it half-way between the $g-c$ and $e-c$ energy gaps (in the simple case of a single relevant c state).

In the two narrow-band pulses setup the central frequency of each pulse can be properly set to address desired non-degenerate states. This is demonstrated in thio-formaldehyde, for which selective preparation of either the T_1 or the T_2 states is obtained. Notably, higher populations for both states are obtained with lower field peak intensities with respect to the single-pulse setup. This is clearly understood by the fact that, for the broadband pulse, a large number of photons are out-of-resonance with either of the two relevant energy gaps ($g-c$ and $e-c$), and only the photons in near resonance with these will promote the process. In the two pulse setups, instead, both the pump and stokes pulses are carefully centered to resonate with the wanted energy-gaps, which allows to use the majority of the photons precisely for the process of interest. This fact not only allows the aforementioned selectivity for non-degenerate states to be realized, but also explains the reduction of

the field peak intensity that is required, with a positive side effect to also reduce loss channels (ionization, Rabi flopping, Stark effect, etc).[37]

In passing, we note that significant room to further enhance the efficiency and selectivity of the described processes is available. In fact, a number of additional field parameters can be controlled, such as the individual pulse shapes, the chirp, the pump and stokes time delay, to name a few. Optimal control can indeed be exploited to improve the viability of the proposed mechanisms and will be the target of a follow-up study.

V. CONCLUSION

To conclude, in this study we propose a stimulated X-ray Raman scattering experiment for the selective population of *optically* dark valence excited states. The approach presented here is more general than currently available approaches, such as two-photon absorption, resonant inelastic X-ray scattering (RIXS) and others (as, e.g., valence states population via autoionizing pathways, ref. [38]). Two-photon absorption can indeed bypass one-photon symmetry selection rules, but it is generally non-selective and would thus produce similar populations in bright and dark states as long as they are degenerate (a situation found in a number of relevant molecular systems, such as DNA and RNA nucleobases); techniques able to address spin-forbidden transitions, such as RIXS[39–44], do not offer the possibility to control the process efficiency and selectivity. Our SXRS based approach allows to access a wider range of dark states in a selective way, bypassing both symmetry and spin selection rules, and relying on the unique properties of core-level spectroscopy: the selectivity of the SXRS process is here investigated providing an intuitive *rule of thumb* based on the *local* symmetry of valence orbital around the excited core-hole and the *spatial overlap* between valence and core molecular orbitals. This simple, but effective picture is the manifestation of the atomic character of core excitation/de-excitation processes.

The ability of the proposed scheme to prepare a system in a superposition of singlet and triplet states directly at the Franck-Condon geometry allows to access and shape coherences that may be exploited as molecular electronic-spin qubits,[1] paving the way for intriguing applications of the proposed technique in quantum computing. For practical applications more suitable molecular systems exhibiting a significantly higher process efficiency are desired[36].

While in this exploratory work we have neglected ionization losses, dephasing effects, and we have assumed a fixed molecular orientation, the introduced concept and its theoretical framework can be straightforwardly extended to account for those without impacting their generality. Finally, as demonstrated, the yield of the proposed processes can be enhanced by suitable manipulation of the employed X-ray fields: this was illustrated by comparing a single broadband pulse setup to pairs of narrow-band pulses, demonstrating that higher yields and selectivity can be achieved in the latter case. This is just the tip of the iceberg, as an ample range of optimal quantum control approaches developed in other spectral windows (as, e.g., STIRAP, that would also lift the problem of the short core-excited state lifetime) can be extended in the X-rays and exploited to maximize the studied processes efficiency, thus facilitating the realization of this novel approach in a number of XFELs and HHG facilites.

ACKNOWLEDGMENTS

F.S. acknowledges financial support from the "Ecosystem for Sustainable Transition in Emilia-Romagna" (ECOSISTER) project, code no. ECS00000033. Support from the U.S. Department of Energy, Office of Science, Office of Basic Energy Sciences, Chemical Sciences, Geosciences and Biosciences Division under award no. DE-SC0022225 is gratefully acknowledged.

[1] D. Jirovec, A. Hofmann, A. Ballabio, P. M. Mutter, G. Tavani, M. Botifoll, A. Crippa, J. Kukucka, O. Sagi, F. Martins, J. Saez-Mollejo, I. Prieto, M. Borovkov, J. Arbiol, D. Chrastina, G. Isella, and G. Katsaros, A singlet-triplet hole spin qubit in planar ge, Nature Materials **20**, 1106 (2021).

[2] A. Nenov, R. Borrego-Varillas, A. Oriana, L. Ganzer, F. Segatta, I. Conti, J. Segarra-Marti, J. Omachi, M. Dapor, S. Taioli, C. Manzoni, S. Mukamel, G. Cerullo, and M. Garavelli, UV-light-induced vibrational coherences: The key to understand kasha rule violation in *trans*-azobenzene, The Journal of Physical Chemistry Letters **9**, 1534 (2018).

[3] T. J. A. Wolf, R. H. Myhre, J. P. Cryan, S. Coriani, R. J. Squibb, A. Battistoni, N. Berrah, C. Bostedt, P. Bucksbaum, G. Coslovich, R. Feifel, K. J. Gaffney, J. Grilj, T. J. Martinez, S. Miyabe, S. P. Moeller, M. Mucke, A. Natan, R. Obaid, T. Osipov, O. Plekan, S. Wang, H. Koch, and M. Gühr, Probing ultrafast $\pi\pi^*/n\pi^*$ internal conversion in organic chromophores via k-edge resonant absorption, Nature Communications **8**, 10.1038/s41467-017-00069-7 (2017).

[4] V. May and O. Kühn, *Charge and Energy Transfer Dynamics in Molecular Systems* (Wiley, 2011).

[5] H. Uoyama, K. Goushi, K. Shizu, H. Nomura, and C. Adachi, Highly efficient organic light-emitting diodes from delayed fluorescence, Nature **492**, 234–238 (2012).

[6] M. A. Baldo, D. F. O'Brien, Y. You, A. Shoustikov, S. Sibley, M. E. Thompson, and S. R. Forrest, Highly efficient phosphorescent emission from organic electroluminescent devices, Nature **395**, 151–154 (1998).

[7] M. Barbatti, A. J. A. Aquino, J. J. Szymczak, D. Nachti-

gallová, P. Hobza, and H. Lischka, Relaxation mechanisms of uv-photoexcited dna and rna nucleobases, Proceedings of the National Academy of Sciences **107**, 21453 (2010).

[8] H. Yu, J. A. Sanchez-Rodriguez, M. Pollum, C. E. Crespo-Hernández, S. Mai, P. Marquetand, L. González, and S. Ullrich, Internal conversion and intersystem crossing pathways in uv excited, isolated uracils and their implications in prebiotic chemistry, Phys. Chem. Chem. Phys. **18**, 20168 (2016).

[9] R. Improta, F. Santoro, and L. Blancafort, Quantum mechanical studies on the photophysics and the photochemistry of nucleic acids and nucleobases, Chemical Reviews **116**, 3540–3593 (2016).

[10] S. Boldissar and M. S. de Vries, How nature covers its bases, Phys. Chem. Chem. Phys. **20**, 9701–9716 (2018).

[11] M. Chergui, M. Beye, S. Mukamel, C. Svetina, and C. Masciovecchio, Progress and prospects in nonlinear extreme-ultraviolet and x-ray optics and spectroscopy, Nature Reviews Physics **5**, 578–596 (2023).

[12] C. P. Schwartz and W. S. Drisdell, Nonlinear soft x-ray spectroscopy, in *Nonlinear X-Ray Spectroscopy for Materials Science* (Springer Nature Singapore, 2023) p. 83–118.

[13] S. Tanaka and S. Mukamel, Coherent x-ray raman spectroscopy: A nonlinear local probe for electronic excitations, Physical Review Letters **89**, 043001 (2002).

[14] N. Rohringer, X-ray raman scattering: a building block for nonlinear spectroscopy, Philosophical Transactions of the Royal Society A: Mathematical, Physical and Engineering Sciences **377**, 20170471 (2019).

[15] C. Weninger, M. Purvis, D. Ryan, R. A. London, J. D. Bozek, C. Bostedt, A. Graf, G. Brown, J. J. Rocca, and N. Rohringer, Stimulated electronic x-ray raman scattering, Physical Review Letters **111**, 10.1103/physrevlett.111.233902 (2013).

[16] T. Pfeifer, Intense x-rays can be (slightly) exciting, Science **369**, 1568–1569 (2020).

[17] Note that the term *overlap* is here used to highlight a situation in which the two orbitals occupy the same region of the 3D space. It does not refer to the overlap integral which, by construction, is zero.

[18] R. Manne, Molecular orbital interpretation of x-ray emission spectra: Simple hydrocarbons and carbon oxides, The Journal of Chemical Physics **52**, 5733 (1970).

[19] S. Mukamel, D. Healion, Y. Zhang, and J. D. Biggs, Multidimensional attosecond resonant x-ray spectroscopy of molecules: Lessons from the optical regime, Annual Review of Physical Chemistry **64**, 101 (2013).

[20] E. Kawerk, S. Carniato, H. Iwayama, E. Shigemasa, M. N. Piancastelli, J. Wassaf, A. Khoury, and M. Simon, Experimental and theoretical study of x-ray absorption around the chlorine l edge in vinyl chloride, Journal of Electron Spectroscopy and Related Phenomena **186**, 1 (2013).

[21] See supplemental material at [. . . url . . .] for model hamiltonian definition, derivation of the equations for both the coherence and population mechanisms, additional details and data about the electronic structure calculations, isxrs selection rules at the $l_{2,3}$ edge, comparison of perturbative and non-perturbative field-matter interaction regimes in a range of field intensities, optimization of the field central frequency for the single broadband field setup, and optimization of the pump and stokes intensities for the two-pulses field setup.

[22] P. A. Malmqvist, A. Rendell, and B. O. Roos, The restricted active space self-consistent-field method, implemented with a split graph unitary group approach, The Journal of Physical Chemistry **94**, 5477 (1990).

[23] P. Å. Malmqvist, K. Pierloot, A. R. M. Shahi, C. J. Cramer, and L. Gagliardi, The restricted active space followed by second-order perturbation theory method: Theory and application to the study of CuO2 and cu2o2 systems, The Journal of Chemical Physics **128**, 204109 (2008).

[24] M. G. Delcey, L. K. Sørensen, M. Vacher, R. C. Couto, and M. Lundberg, Efficient calculations of a large number of highly excited states for multiconfigurational wavefunctions, Journal of Computational Chemistry **40**, 1789 (2019).

[25] D. Peng and M. Reiher, Exact decoupling of the relativistic fock operator, Theoretical Chemistry Accounts **131**, 10.1007/s00214-011-1081-y (2012).

[26] J. M. Kasper, T. F. Stetina, A. J. Jenkins, and X. Li, Ab initio methods for l-edge x-ray absorption spectroscopy, Chemical Physics Reviews **1**, 10.1063/5.0029725 (2020).

[27] I. F. Galván, M. Vacher, A. Alavi, C. Angeli, F. Aquilante, J. Autschbach, J. J. Bao, S. I. Bokarev, N. A. Bogdanov, R. K. Carlson, L. F. Chibotaru, J. Creutzberg, N. Dattani, M. G. Delcey, S. S. Dong, A. Dreuw, L. Freitag, L. M. Frutos, L. Gagliardi, F. Gendron, A. Giussani, L. González, G. Grell, M. Guo, C. E. Hoyer, M. Johansson, S. Keller, S. Knecht, G. Kovačević, E. Källman, G. L. Manni, M. Lundberg, Y. Ma, S. Mai, J. P. Malhado, P. Å. Malmqvist, P. Marquetand, S. A. Mewes, J. Norell, M. Olivucci, M. Oppel, Q. M. Phung, K. Pierloot, F. Plasser, M. Reiher, A. M. Sand, I. Schapiro, P. Sharma, C. J. Stein, L. K. Sørensen, D. G. Truhlar, M. Ugandi, L. Ungur, A. Valentini, S. Vancoillie, V. Veryazov, O. Weser, T. A. Wesołowski, P.-O. Widmark, S. Wouters, A. Zech, J. P. Zobel, and R. Lindh, OpenMolcas: From source code to insight, Journal of Chemical Theory and Computation **15**, 5925 (2019).

[28] F. Aquilante, J. Autschbach, A. Baiardi, S. Battaglia, V. A. Borin, L. F. Chibotaru, I. Conti, L. D. Vico, M. Delcey, I. F. Galván, N. Ferré, L. Freitag, M. Garavelli, X. Gong, S. Knecht, E. D. Larsson, R. Lindh, M. Lundberg, P. Å. Malmqvist, A. Nenov, J. Norell, M. Odelius, M. Olivucci, T. B. Pedersen, L. Pedraza-González, Q. M. Phung, K. Pierloot, M. Reiher, I. Schapiro, J. Segarra-Martí, F. Segatta, L. Seijo, S. Sen, D.-C. Sergentu, C. J. Stein, L. Ungur, M. Vacher, A. Valentini, and V. Veryazov, Modern quantum chemistry with [open]molcas, The Journal of Chemical Physics **152**, 214117 (2020).

[29] G. Li Manni, I. Fdez. Galván, A. Alavi, F. Aleotti, F. Aquilante, J. Autschbach, D. Avagliano, A. Baiardi, J. J. Bao, S. Battaglia, L. Birnoschi, A. Blanco-González, S. I. Bokarev, R. Broer, R. Cacciari, P. B. Calio, R. K. Carlson, R. Carvalho Couto, L. Cerdán, L. F. Chibotaru, N. F. Chilton, J. R. Church, I. Conti, S. Coriani, J. Cuéllar-Zuquin, R. E. Daoud, N. Dattani, P. Decleva, C. de Graaf, M. G. Delcey, L. De Vico, W. Dobrautz, S. S. Dong, R. Feng, N. Ferré, M. Filatov(Gulak), L. Gagliardi, M. Garavelli, L. González, Y. Guan, M. Guo, M. R. Hennefarth, M. R. Hermes, C. E. Hoyer, M. Huix-Rotllant, V. K. Jaiswal, A. Kaiser,

D. S. Kaliakin, M. Khamesian, D. S. King, V. Kochetov, M. Krośnicki, A. A. Kumaar, E. D. Larsson, S. Lehtola, M.-B. Lepetit, H. Lischka, P. López Ríos, M. Lundberg, D. Ma, S. Mai, P. Marquetand, I. C. D. Merritt, F. Montorsi, M. Mörchen, A. Nenov, V. H. A. Nguyen, Y. Nishimoto, M. S. Oakley, M. Olivucci, M. Oppel, D. Padula, R. Pandharkar, Q. M. Phung, F. Plasser, G. Raggi, E. Rebolini, M. Reiher, I. Rivalta, D. Roca-Sanjuán, T. Romig, A. A. Safari, A. Sánchez-Mansilla, A. M. Sand, I. Schapiro, T. R. Scott, J. Segarra-Martí, F. Segatta, D.-C. Sergentu, P. Sharma, R. Shepard, Y. Shu, J. K. Staab, T. P. Straatsma, L. K. Sørensen, B. N. C. Tenorio, D. G. Truhlar, L. Ungur, M. Vacher, V. Veryazov, T. A. Voß, O. Weser, D. Wu, X. Yang, D. Yarkony, C. Zhou, J. P. Zobel, and R. Lindh, The openmolcas web: A community-driven approach to advancing computational chemistry, Journal of Chemical Theory and Computation **19**, 6933–6991 (2023).

[30] J. Johansson, P. Nation, and F. Nori, QuTiP: An open-source python framework for the dynamics of open quantum systems, Computer Physics Communications **183**, 1760 (2012).

[31] J. Johansson, P. Nation, and F. Nori, QuTiP 2: A python framework for the dynamics of open quantum systems, Computer Physics Communications **184**, 1234 (2013).

[32] J. T. O'Neal, E. G. Champenois, S. Oberli, R. Obaid, A. Al-Haddad, J. Barnard, N. Berrah, R. Coffee, J. Duris, G. Galinis, D. Garratt, J. M. Glownia, D. Haxton, P. Ho, S. Li, X. Li, J. MacArthur, J. P. Marangos, A. Natan, N. Shivaram, D. S. Slaughter, P. Walter, S. Wandel, L. Young, C. Bostedt, P. H. Bucksbaum, A. Picón, A. Marinelli, and J. P. Cryan, Electronic population transfer via impulsive stimulated x-ray raman scattering with attosecond soft-x-ray pulses, Physical Review Letters **125**, 073203 (2020).

[33] M. F. Gelin, L. Chen, and W. Domcke, Equation-of-motion methods for the calculation of femtosecond time-resolved 4-wave-mixing and n-wave-mixing signals, Chemical Reviews **122**, 17339 (2022).

[34] Note that the process that brings the electron back to the ground state, captured by ϱ_{gg}, is also possible. Nonetheless, since the focus here is on excited states, we will not explicitly discuss this pathway.

[35] S. Mukamel, *Principles of Nonlinear Optical Spectroscopy* (Oxford University Press, New York, 1995).

[36] L. Oberti, L. Avaldi, P. Bolognesi, M. Bonanomi, R. Borrego-Varillas, C. Callegari, L. Carlini, E. Ciekalski, M. Coreno, M. Devetta, M. Di Fraia, M. Garavelli, M. Goffe, C. Grazioli, F. Montorsi, K. C. Prince, R. Richter, F. Segatta, S. Waldmannstetter, G. Cerullo, H. Dube, O. Plekan, D. Faccialá, C. Vozzi, and A. Nenov, Probing the electronic structure of hemithioindigo photoswitches and their different substituents, Submitted (2024).

[37] J. P. Cryan, T. Driver, J. Duris, Z. Guo, S. Li, J. T. O'Neal, and A. Marinelli, The development of attosecond xfels for understanding ultrafast electron motion, in *Advances in Atomic, Molecular, and Optical Physics* (Elsevier, 2022) p. 1–64.

[38] M. Singh, M. A. Fareed, V. Birulia, A. Magunov, A. N. Grum-Grzhimailo, P. Lassonde, A. Laramée, R. Marcelino, R. G. Shirinabadi, F. Légaré, T. Ozaki, and V. Strelkov, Ultrafast resonant state formation by the coupling of rydberg and dark autoionizing states, Physical Review Letters **130**, 073201 (2023).

[39] H. Lu, M. Rossi, A. Nag, M. Osada, D. F. Li, K. Lee, B. Y. Wang, M. Garcia-Fernandez, S. Agrestini, Z. X. Shen, E. M. Been, B. Moritz, T. P. Devereaux, J. Zaanen, H. Y. Hwang, K.-J. Zhou, and W. S. Lee, Magnetic excitations in infinite-layer nickelates, Science **373**, 213–216 (2021).

[40] A. Nag, H. Robarts, F. Wenzel, J. Li, H. Elnaggar, R.-P. Wang, A. Walters, M. García-Fernández, F. de Groot, M. Haverkort, and K.-J. Zhou, Many-body physics of single and double spin-flip excitations in nio, Physical Review Letters **124**, 10.1103/physrevlett.124.067202 (2020).

[41] B. E. Van Kuiken, A. W. Hahn, D. Maganas, and S. DeBeer, Measuring spin-allowed and spin-forbidden d–d excitations in vanadium complexes with 2p3d resonant inelastic x-ray scattering, Inorganic Chemistry **55**, 11497–11501 (2016).

[42] A. W. Hahn, B. E. Van Kuiken, V. G. Chilkuri, N. Levin, E. Bill, T. Weyhermüller, A. Nicolaou, J. Miyawaki, Y. Harada, and S. DeBeer, Probing the valence electronic structure of low-spin ferrous and ferric complexes using 2p3d resonant inelastic x-ray scattering (rixs), Inorganic Chemistry **57**, 9515–9530 (2018).

[43] A. W. Hahn, B. E. Van Kuiken, M. al Samarai, M. Atanasov, T. Weyhermüller, Y.-T. Cui, J. Miyawaki, Y. Harada, A. Nicolaou, and S. DeBeer, Measurement of the ligand field spectra of ferrous and ferric iron chlorides using 2p3d rixs, Inorganic Chemistry **56**, 8203–8211 (2017).

[44] B. E. Van Kuiken, A. W. Hahn, B. Nayyar, C. E. Schiewer, S. C. Lee, F. Meyer, T. Weyhermüller, A. Nicolaou, Y.-T. Cui, J. Miyawaki, Y. Harada, and S. DeBeer, Electronic spectra of iron–sulfur complexes measured by 2p3d rixs spectroscopy, Inorganic Chemistry **57**, 7355–7361 (2018).